NJC

PAPER

View Article Online
View Journal | View Issue

Alkane oxidation with peroxides catalyzed by cage-like copper(II) silsesquioxanes

Mikhail M. Vinogradov, [ac] Yuriy N. Kozlov, [b] Alexey N. Bilyachenko, [a] Dmytro S. Nesterov, [c] Lidia S. Shul'pina, [a] Yan V. Zubavichus, [ad] Armando J. L. Pombeiro, [c] Mikhail M. Levitsky, [a] Alexey I. Yalymov [a] and Georgiy B. Shul'pin *[b]

[a] *Nesmeyanov Institute of Organoelement Compounds, Russian Academy of Sciences, ulitsa Vavilova, dom 28, Moscow 119991, Russia*
[b] *Semenov Institute of Chemical Physics, Russian Academy of Sciences, ulitsa Kosygina, dom 4, Moscow 119991, Russia*
[c] *Centro de Química Estrutural, Complexo I, Instituto Superior Técnico, Universidade de Lisboa, Av. Rovisco Pais, 1049-001 Lisboa, Portugal*
[d] *National Research Center "Kurchatov Institute", pl. Akad. Kurchatova, dom 1, Moscow 123098, Russia*

* Corresponding author. Tel.: +7 495 9397317; fax: +7499 1376130; +7495 6512191; *e-mail addresses:* Shulpin@chph.ras.ru and gbsh@mail.ru (G. B. Shul'pin)

Supplementary information

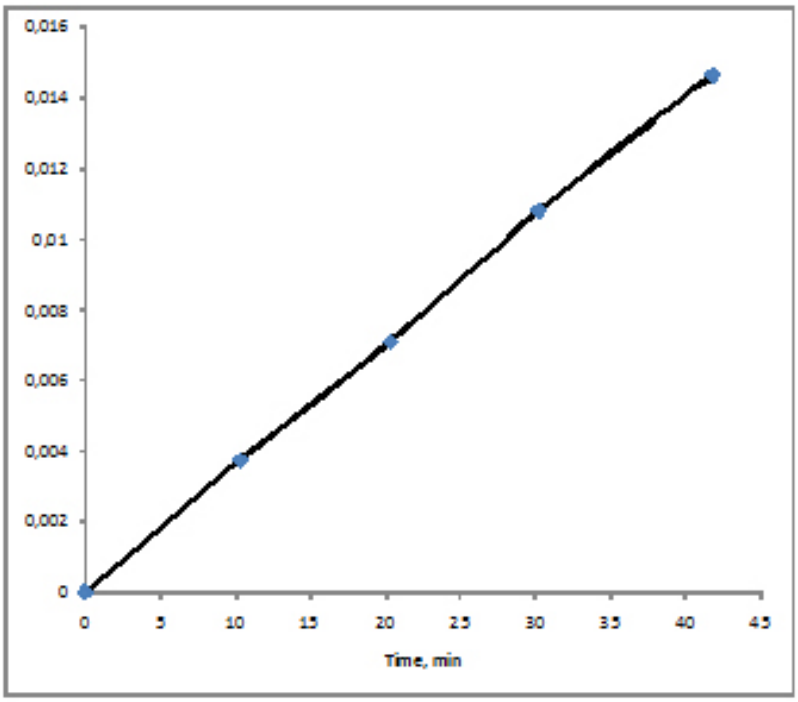

$[\mathbf{1a}]_0 = 1.86 \times 10^{-4}$ M

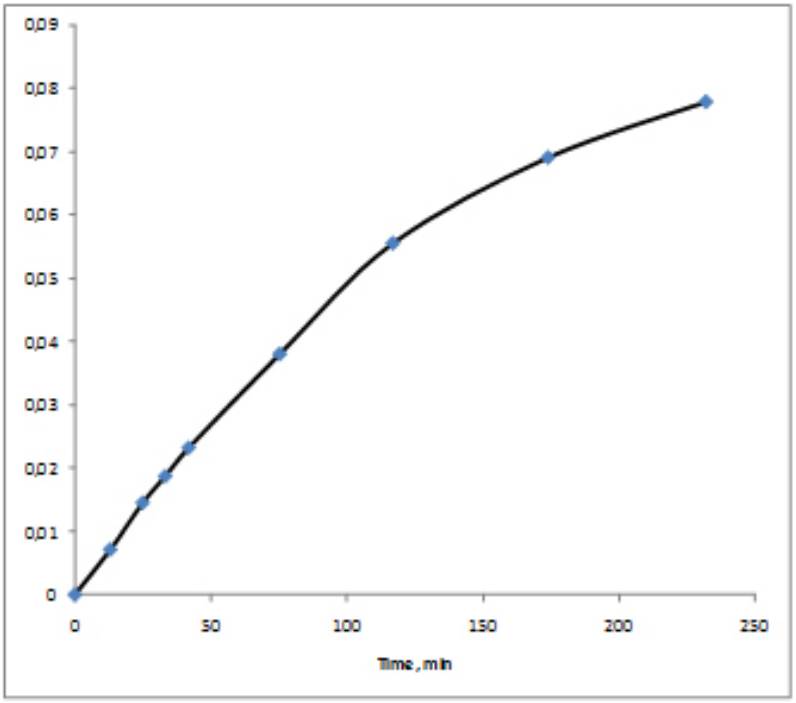

$[\mathbf{1a}]_0 = 4.12 \times 10^{-4}$ M

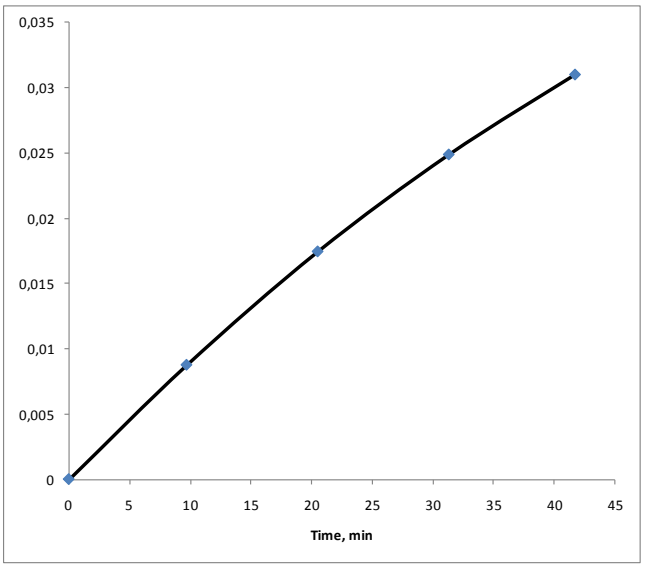

$[\mathbf{1a}]_0 = 6.33 \times 10^{-4}$ M

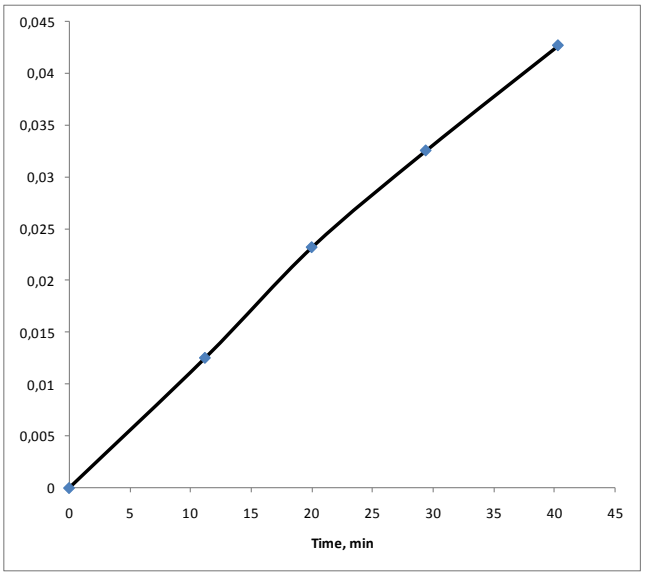

$[\mathbf{1a}]_0 = 8.54 \times 10^{-4}$ M

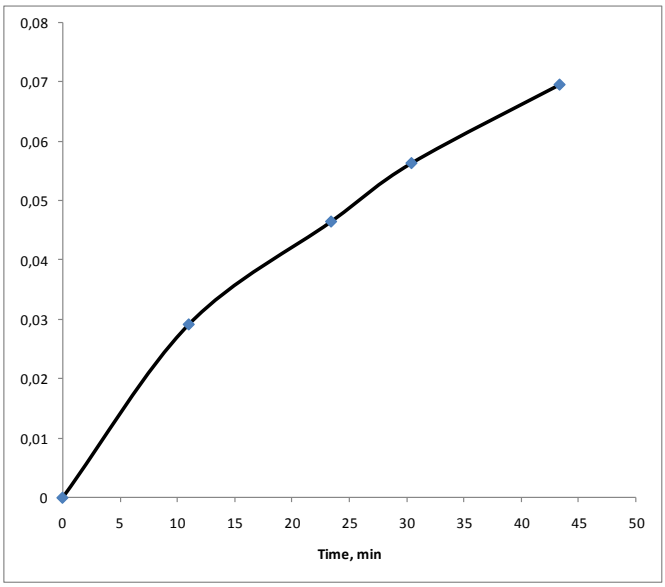

$[\mathbf{1a}]_0 = 17.6 \times 10^{-4}$ M

Fig. S1. Oxidation of cyclohexane with H_2O_2 catalyzed by complex **1a** at its different concentrations. Accumulation of a sum (concentration, M) of products (cyclohexyl hydroperoxide, cyclohexanone and cyclohexanol) with time is shown. Conditions: catalyst **1a** (4.12×10^{-4} M corresponds to 5.3 mg), $[\text{cyclohexane}]_0 = 0.46$ M (0.25 mL), $[H_2O_2]_0 = 1.0$ M (50% aqueous; 0.29 mL), $[H_2O]_{total} = 2.65$ M, $[HNO_3]_0 = 0.4$ M (65%; 0.19 g), solvent MeCN (total volume of the reaction solution was 5 mL), 60 °C. Concentrations of the products (cyclohexanol and cyclohexanone) were measured after reduction with PPh_3. Dependence of the initial reaction rate W_0 on initial concentration of complex **1a** is shown in Fig. 5.

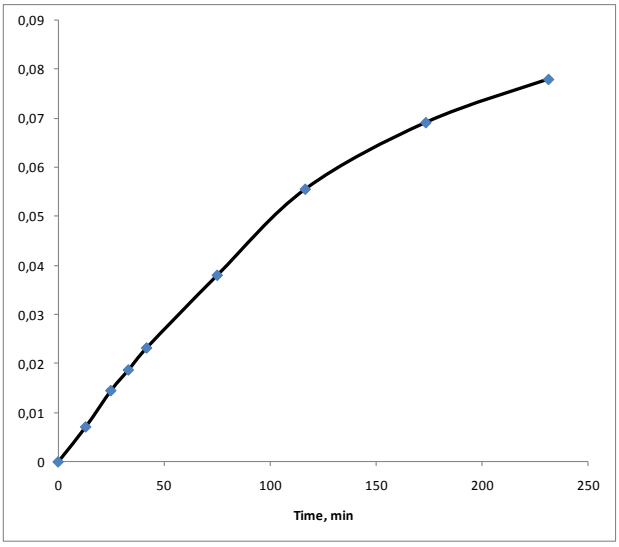

$[HNO_3]_0$ = 0.4 M

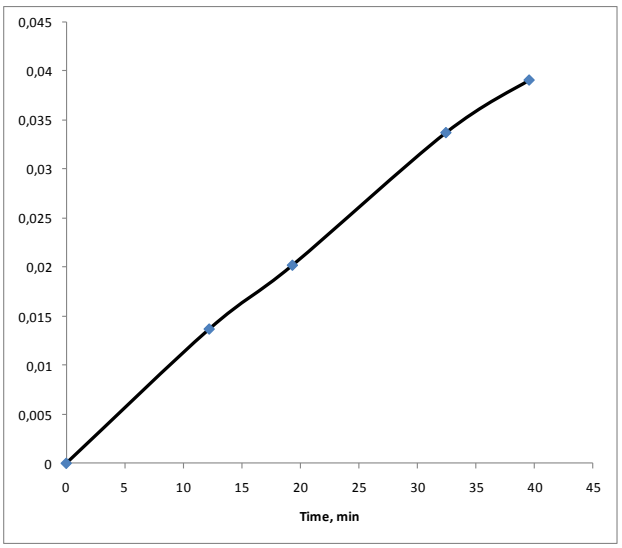

$[HNO_3]_0$ = 0.8 M

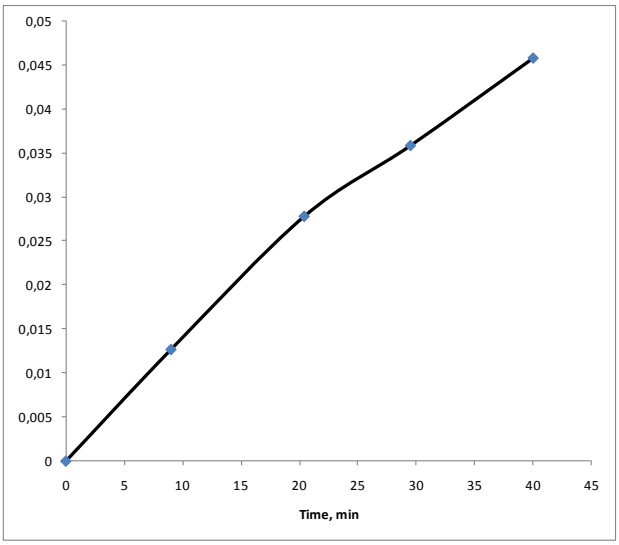

$[HNO_3]_0$ = 1.2 M

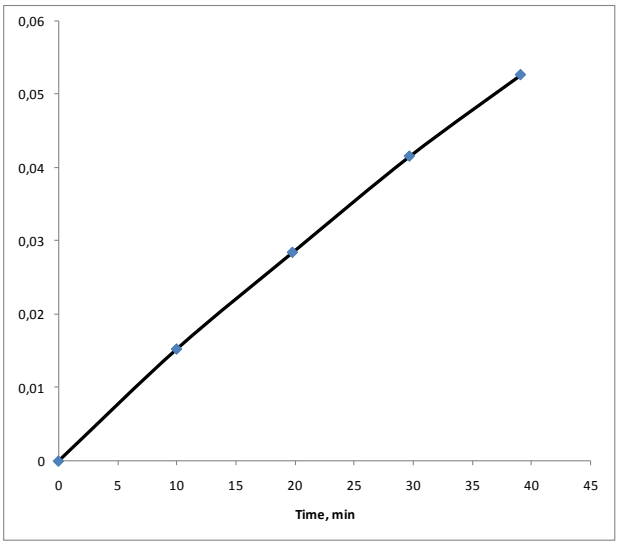

$[HNO_3]_0$ = 1.6 M

Fig. S2. Oxidation of cyclohexane with H_2O_2 catalyzed by complex **1a** at different concentrations of added nitric acid. Accumulation of a sum (concentration, M) of products (cyclohexyl hydroperoxide, cyclohexanone and cyclohexanol) with time is shown. Conditions: $[\mathbf{1a}]_0 = 4.1 \times 10^{-4}$ M, $[\text{cyclohexane}]_0$ = 0.46 M, $[H_2O_2]_0$ = 1.0 M (50% aqueous), $[H_2O]_{total}$ = 2.65 M, solvent MeCN, 60 °C. Concentrations of the products (cyclohexanol and cyclohexanone) were measured after reduction with PPh_3. Dependence of the initial reaction rate W_0 on concentration of added HNO_3 is shown in Fig. 6.

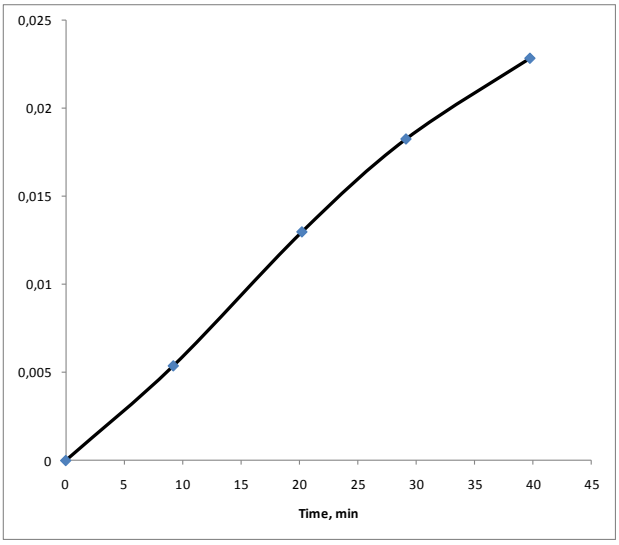

$[H_2O_2]_0 = 0.5$ M

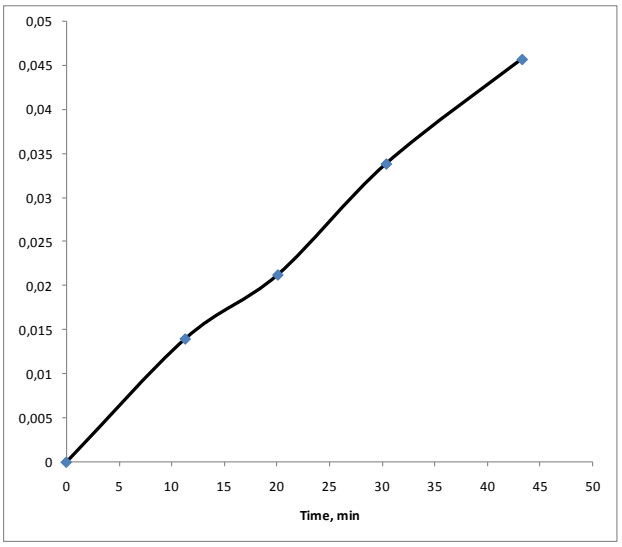

$[H_2O_2]_0 = 1.0$ M

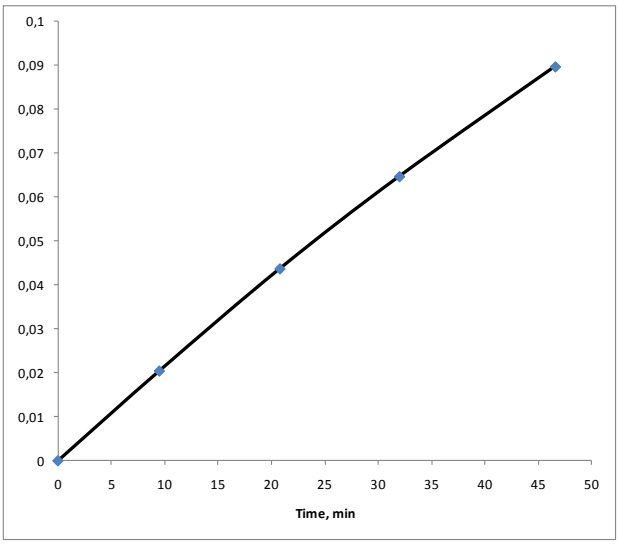

$[H_2O_2]_0 = 2.0$ M

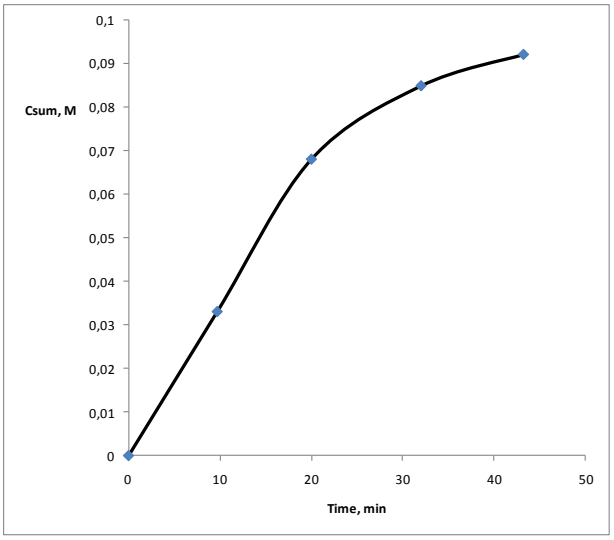

$[H_2O_2]_0 = 3.0$ M

Fig. S3. Oxidation of cyclohexane with H_2O_2 catalyzed by complex **1a** at different concentrations of hydrogen peroxide (50% aqueous). Accumulation of a sum (concentration, M) of products (cyclohexyl hydroperoxide, cyclohexanone and cyclohexanol) with time is shown. Conditions: $[\mathbf{1}]_0 = 4.1 \times 10^{-4}$ M, $[\text{cyclohexane}]_0 = 0.46$ M, $[H_2O]_{total} = const = 2.65$ M, $[HNO_3]_0 = 0.4$ M, solvent MeCN, 60 °C. Concentrations of the products (cyclohexanol and cyclohexanone) were measured after reduction with PPh_3. Dependence of the initial reaction rate W_0 on concentration of H_2O_2 is shown in Fig. 7.

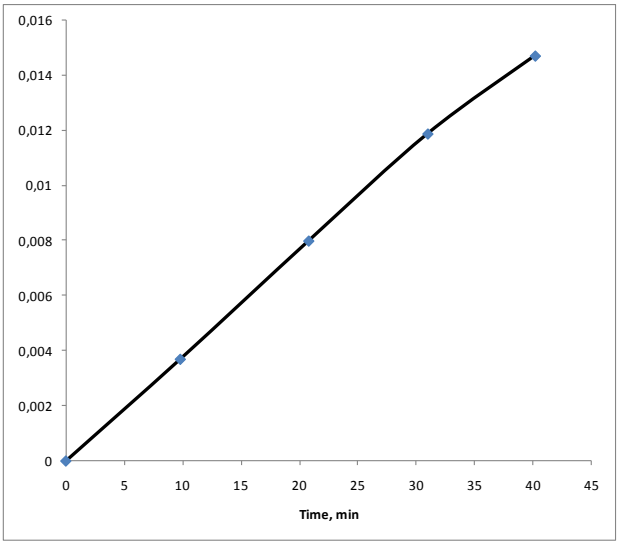

$[cyclohexane]_0 = 0.17$ M

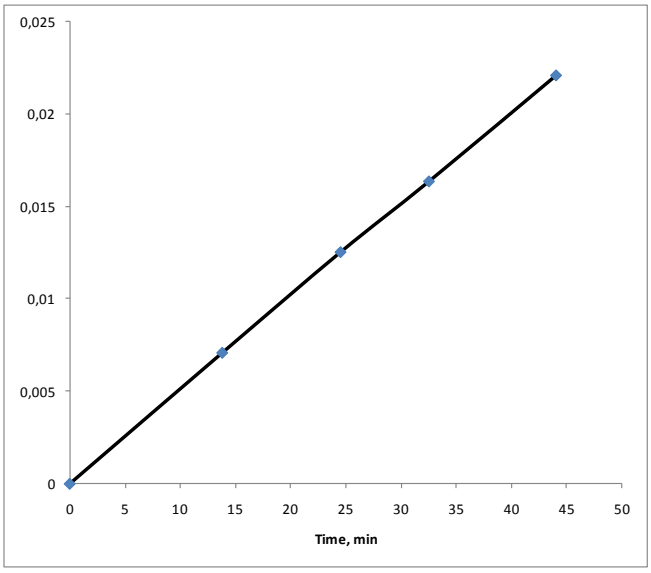

$[cyclohexane]_0 = 0.32$ M

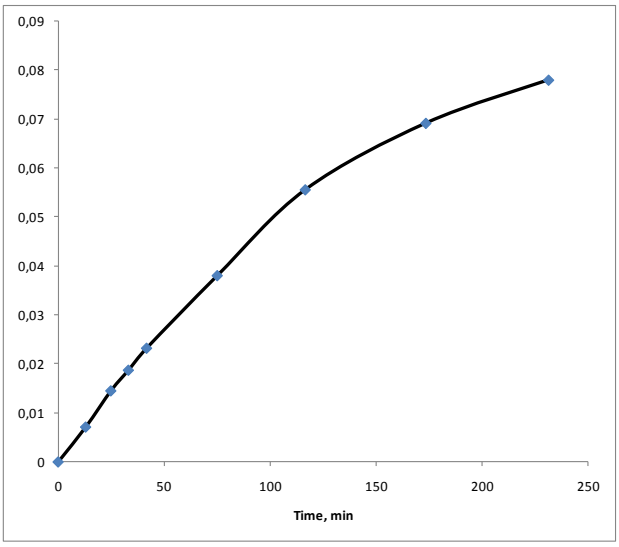

$[cyclohexane]_0 = 0.46$ M

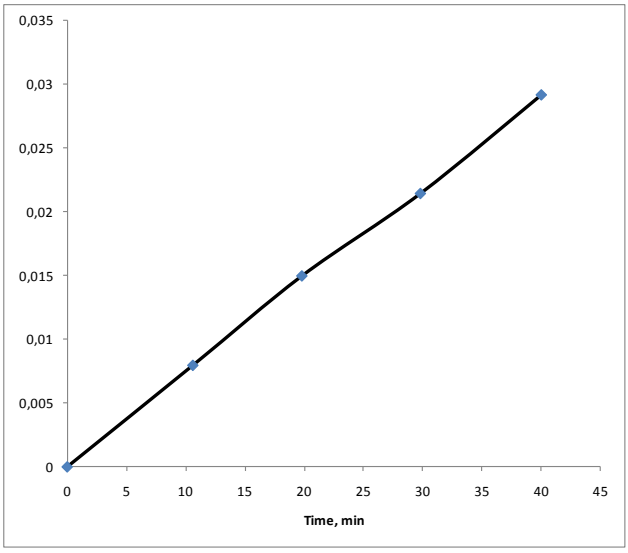

$[cyclohexane]_0 = 0.70$ M

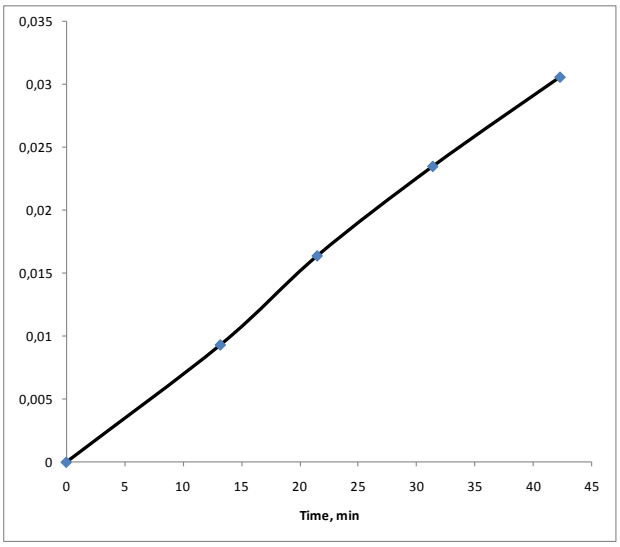

$[cyclohexane]_0 = 0.90$ M

Fig. S4. Oxidation of cyclohexane with H_2O_2 catalyzed by complex **1a** at different initial concentrations of cyclohexane. Accumulation of a sum (concentration, M) of products (cyclohexyl hydroperoxide, cyclohexanone and cyclohexanol) with time is shown. Conditions: $[\mathbf{1a}]_0 = 4.1 \times 10^{-4}$ M, $[H_2O_2]_0 = 1.0$ M (50% aqueous), $[H_2O]_{total} = 2.65$ M, $[HNO_3]_0 = 0.4$ M, solvent MeCN, 60 °C. Concentrations of the products (cyclohexanol and cyclohexanone) were measured after reduction with PPh_3. Dependence of the initial reaction rate W_0 on initial concentration of cycohexane is shown in Fig. 8.

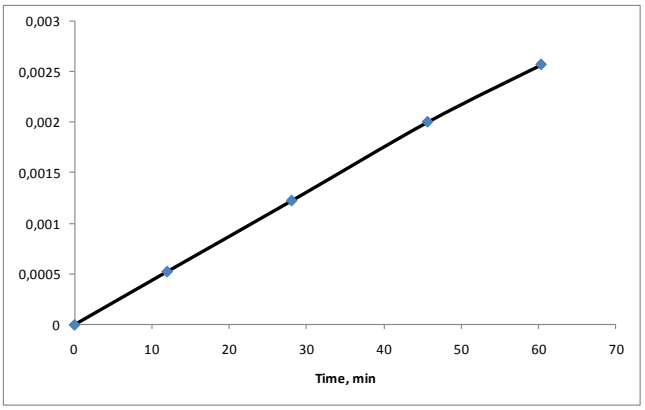

Temperature 30 °C.

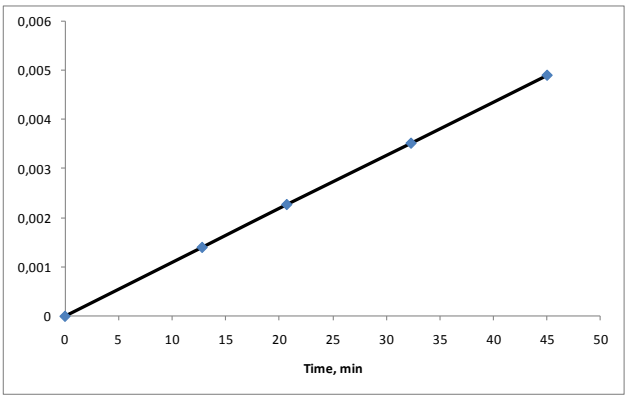

Temperature 40 °C.

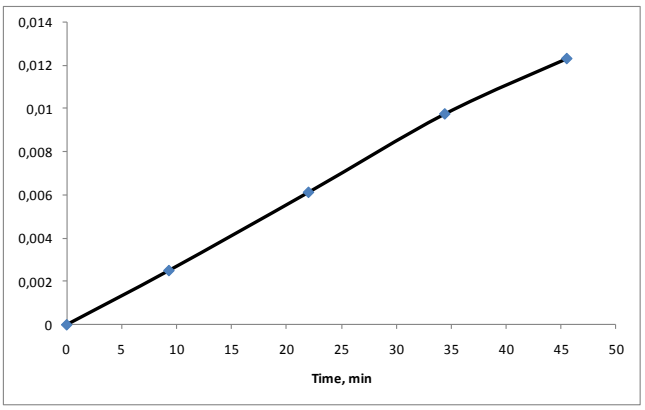

Temperature 50 °C.

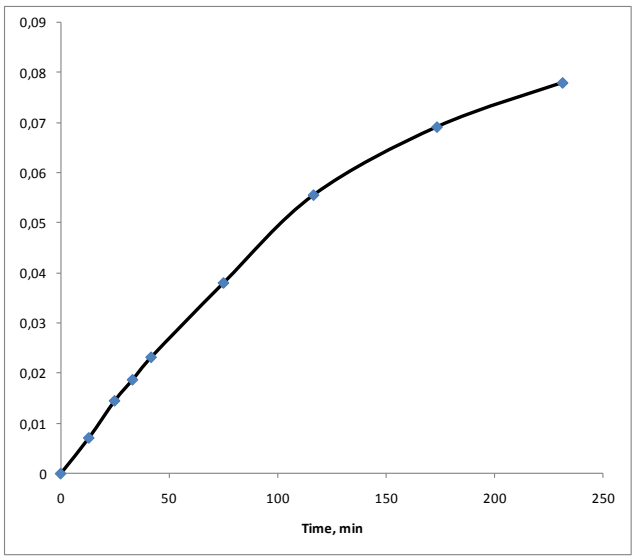

Temperature 60 °C.

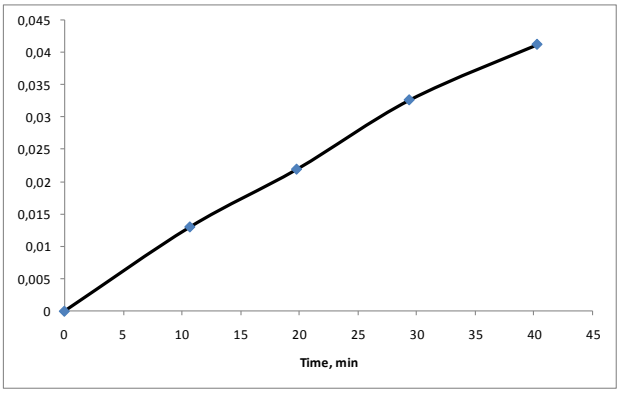

Temperature 70 °C.

Fig. S5. Oxidation of cyclohexane with H_2O_2 catalyzed by complex **1a** at different temperatures. Accumulation of a sum (concentration, M) of products (cyclohexyl hydroperoxide, cyclohexanone and cyclohexanol) with time is shown. Conditions: $[\mathbf{1}]_0 = 4.1 \times 10^{-4}$ M, $[\text{cyclohexane}]_0 = 0.46$ M, $[H_2O_2]_0 = 1.0$ M (50% aqueous), $[H_2O]_{total} = 2.65$ M, $[HNO_3]_0 = 0.4$ M, solvent MeCN. Concentrations of the products (cyclohexanol and cyclohexanone) were measured after reduction with PPh_3. The Arrhenius plot is presented in Fig. S6. This dependence corresponds to the effective activation energy $E_a = 16 \pm 2$ kcal mol^{-1}.

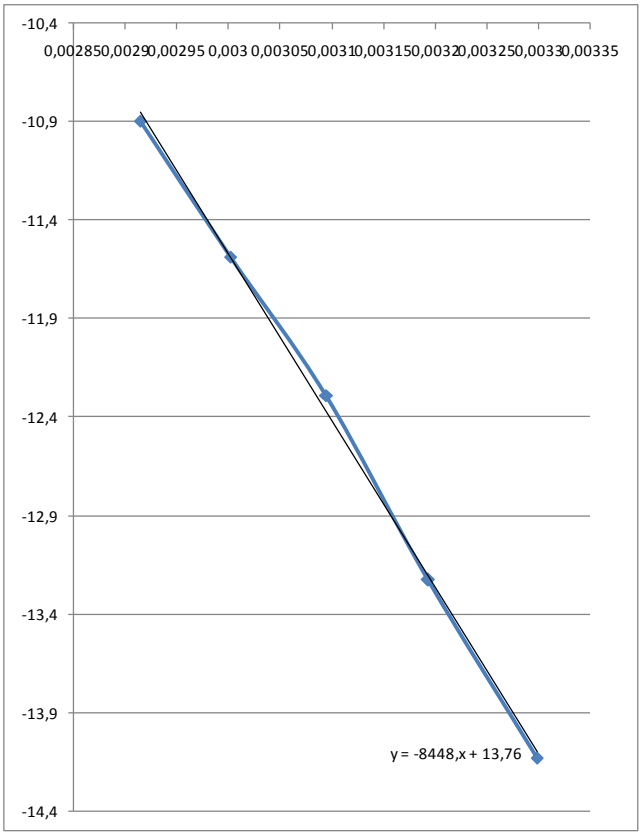

Fig. S6. The Arrhenius plot for the cyclohexane oxidation with H_2O_2 catalyzed by complex **1a** (for conditions, see Fig. S5). This dependence corresponds to the effective activation energy $E_a = 16 \pm 2$ kcal mol^{-1}. The original kinetic curves at different temperatures are presented in Fig. S5.

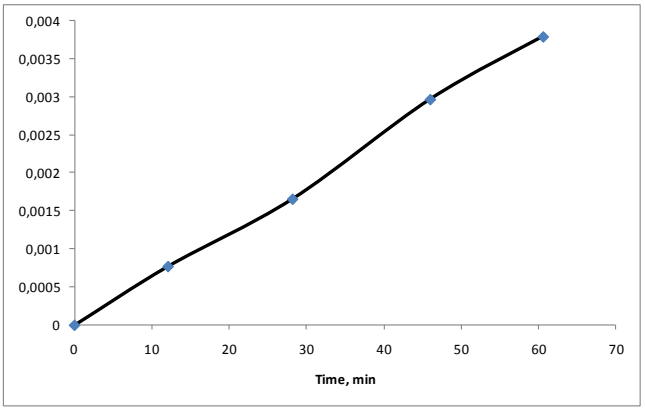

Temperature 30 °C.

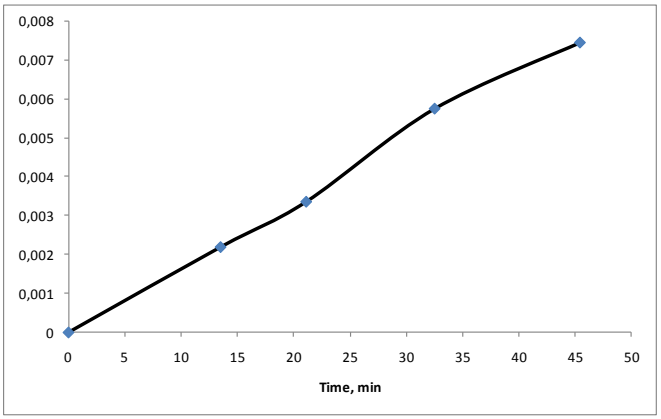

Temperature 40 °C.

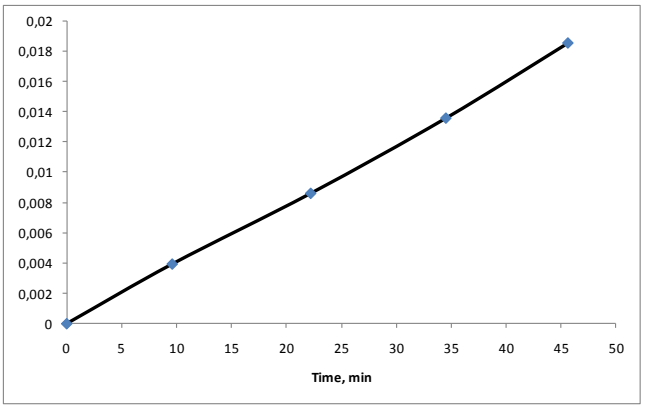

Temperature 50 °C.

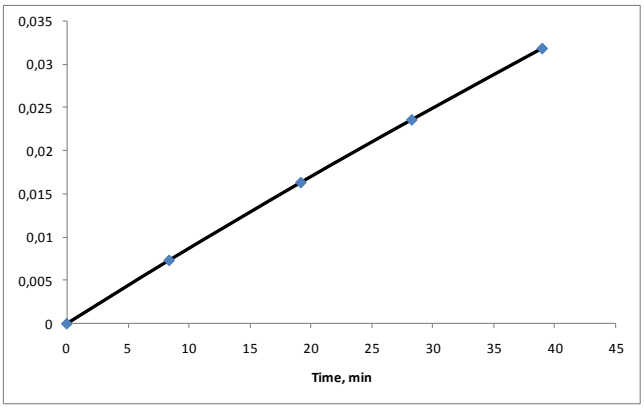

Temperature 60 °C.

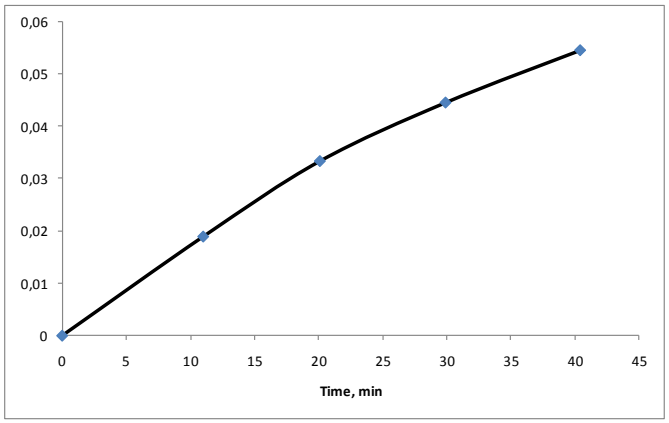

Temperature 60 °C.

Fig. S7. Oxidation of cyclohexane with H_2O_2 catalyzed by complex **2** at different temperatures. Accumulation of a sum (concentration, M) of products (cyclohexyl hydroperoxide, cyclohexanone and cyclohexanol) with time is shown. Conditions: $[\mathbf{2}]_0 = 8.2 \times 10^{-4}$ M, $[\text{cyclohexane}]_0 = 0.46$ M, $[H_2O_2]_0 = 1.0$ M (50% aqueous), $[H_2O]_{total} = 2.65$ M, $[HNO_3]_0 = 0.4$ M, solvent MeCN. Concentrations of the products (cyclohexanol and cyclohexanone) were measured after reduction with PPh_3. The Arrhenius plot is presented in Fig. S8. This dependence corresponds to the effective activation energy $E_a = 17 \pm 2$ kcal mol^{-1}.

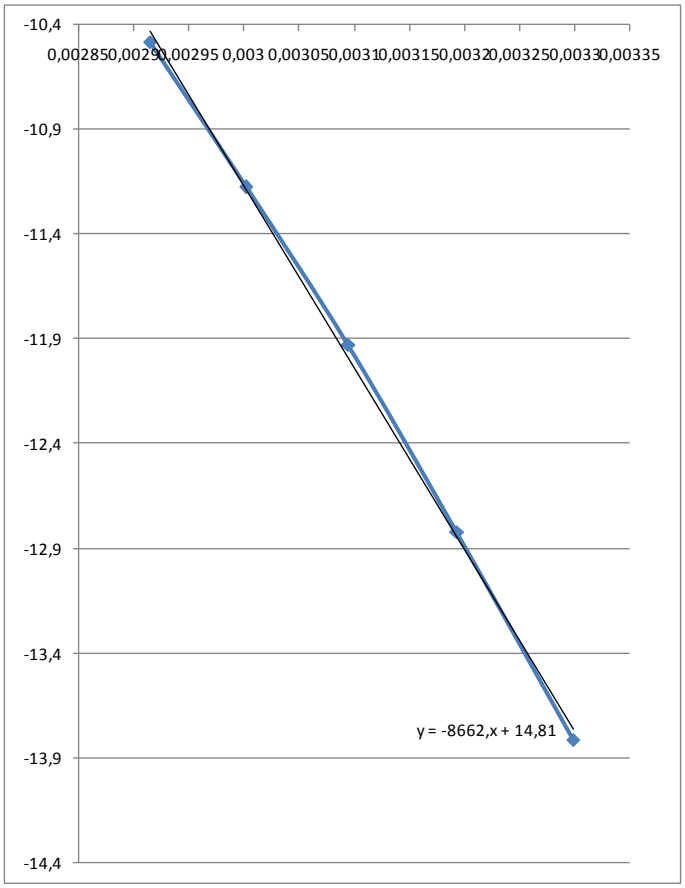

Fig. S8. The Arrhenius plot for the cyclohexane oxidation with H_2O_2 catalyzed by complex **2** (for conditions, see Fig. S7). This dependence corresponds to the effective activation energy E_a = 17 ± 2 kcal mol^{-1}. The original kinetic curves at different temperatures are presented in Fig. S7.

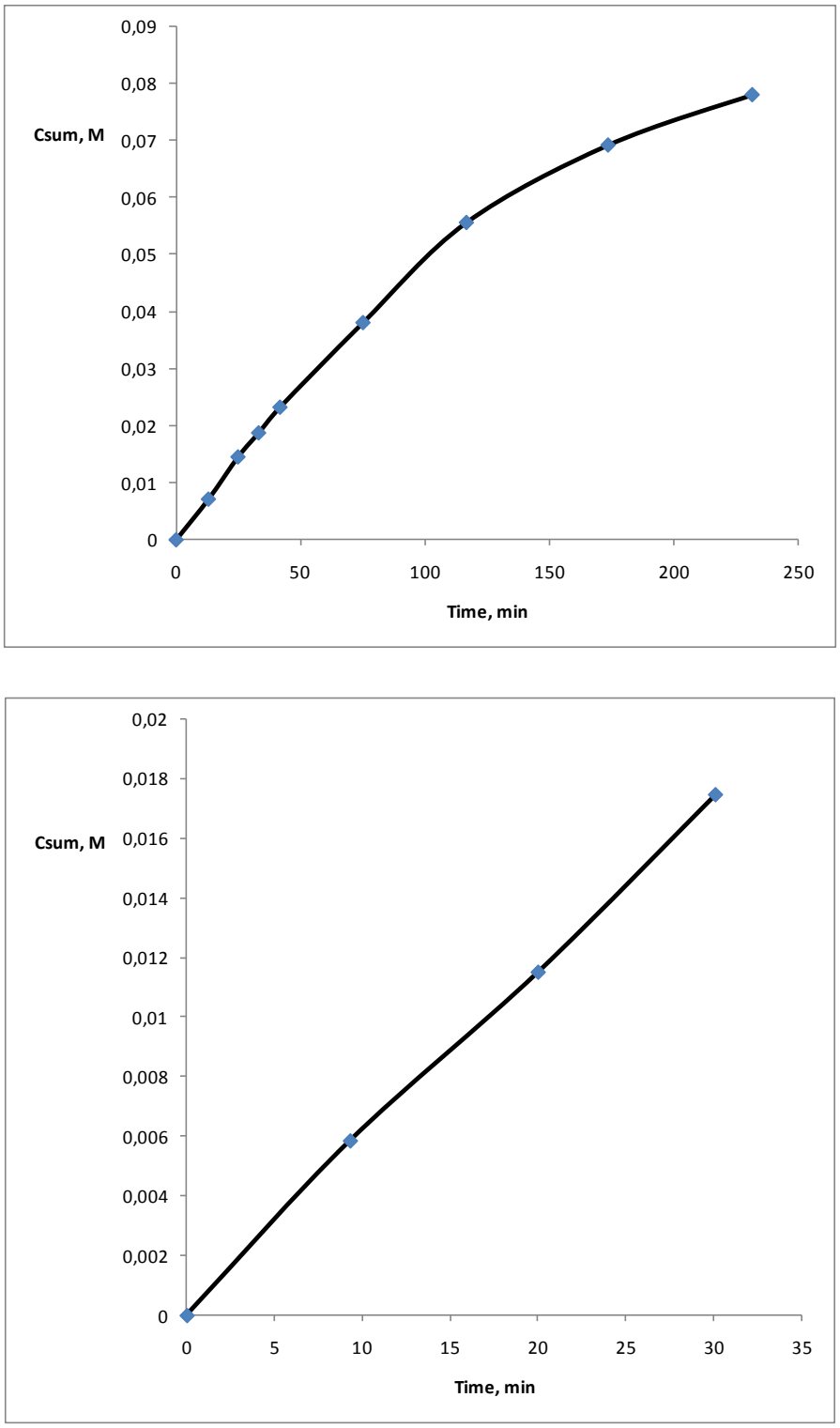

Fig. S9. Oxidation of cyclohexane with H_2O_2 catalyzed by complex **1a** in the absence of benzene (top) and in the presence (0.02 M; bottom) of benzene. Accumulation of a sum (concentration, M) of products (cyclohexyl hydroperoxide, cyclohexanone and cyclohexanol) with time is shown. Conditions: $[\mathbf{1a}]_0 = 4.1 \times 10^{-4}$ M, $[\text{cyclohexane}]_0 = 0.46$ M, $[H_2O_2]_0 = 1.0$ M (50% aqueous), $[H_2O]_{total} = 2.65$ M, $[HNO_3]_0 = 0.4$ M, solvent MeCN. Concentrations of the products (cyclohexanol and cyclohexanone) were measured after reduction with PPh_3.

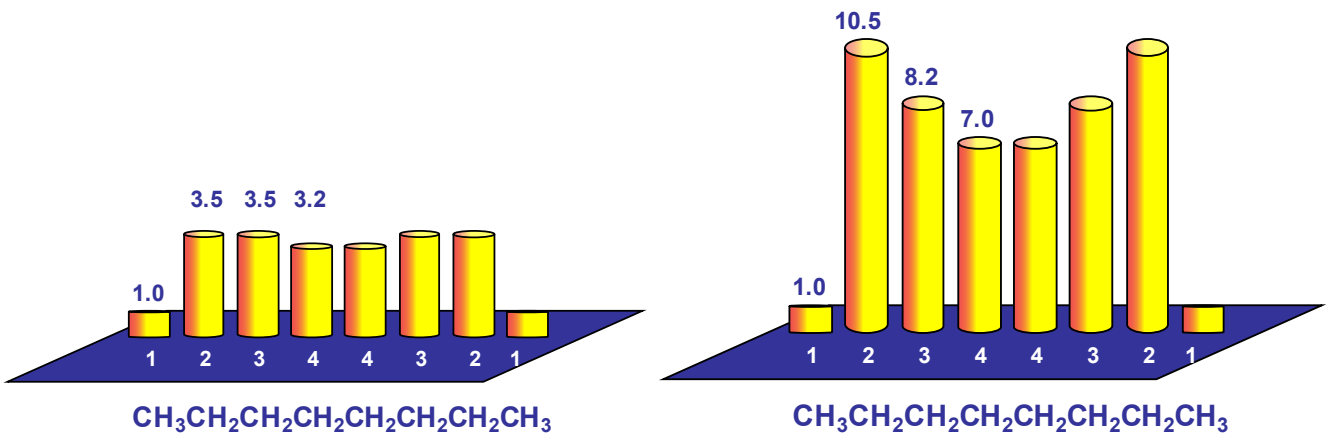

Fig. S10. Isomer distribution in the *n*-octane oxidation with H_2O_2 (left graph) and TBHP (right graph) catalyzed by complex **1a** (see also Table 2, entries 1 and 3).

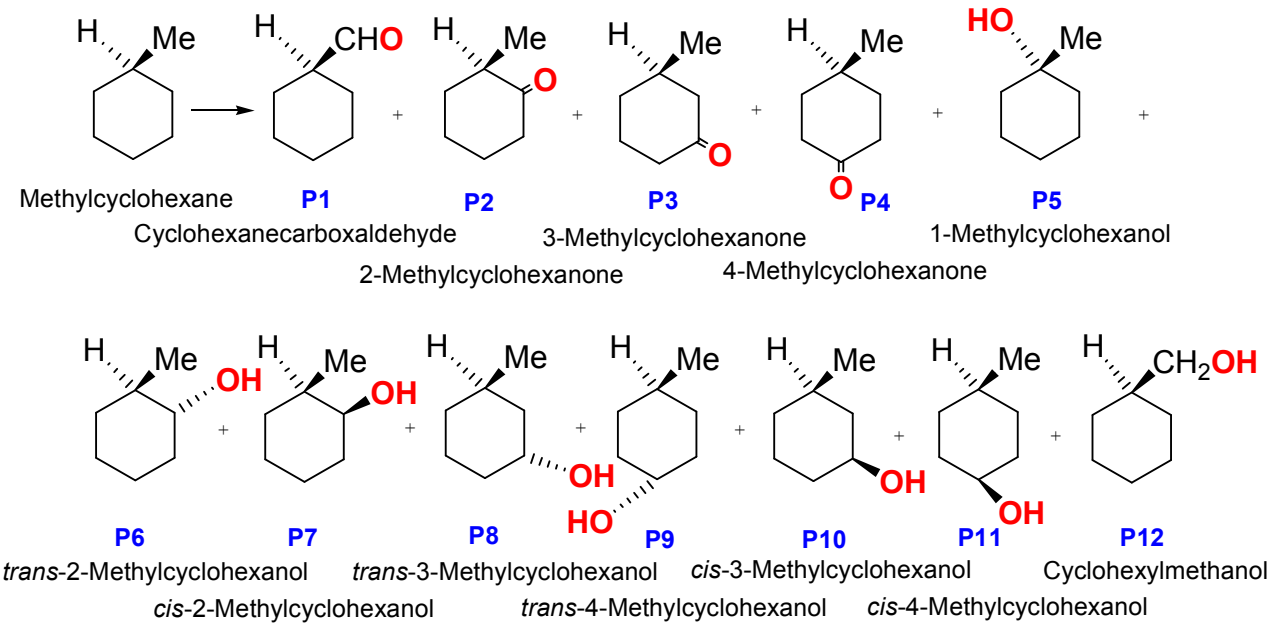

Fig. S11. Products obtained in the methylcyclohexane oxidation.

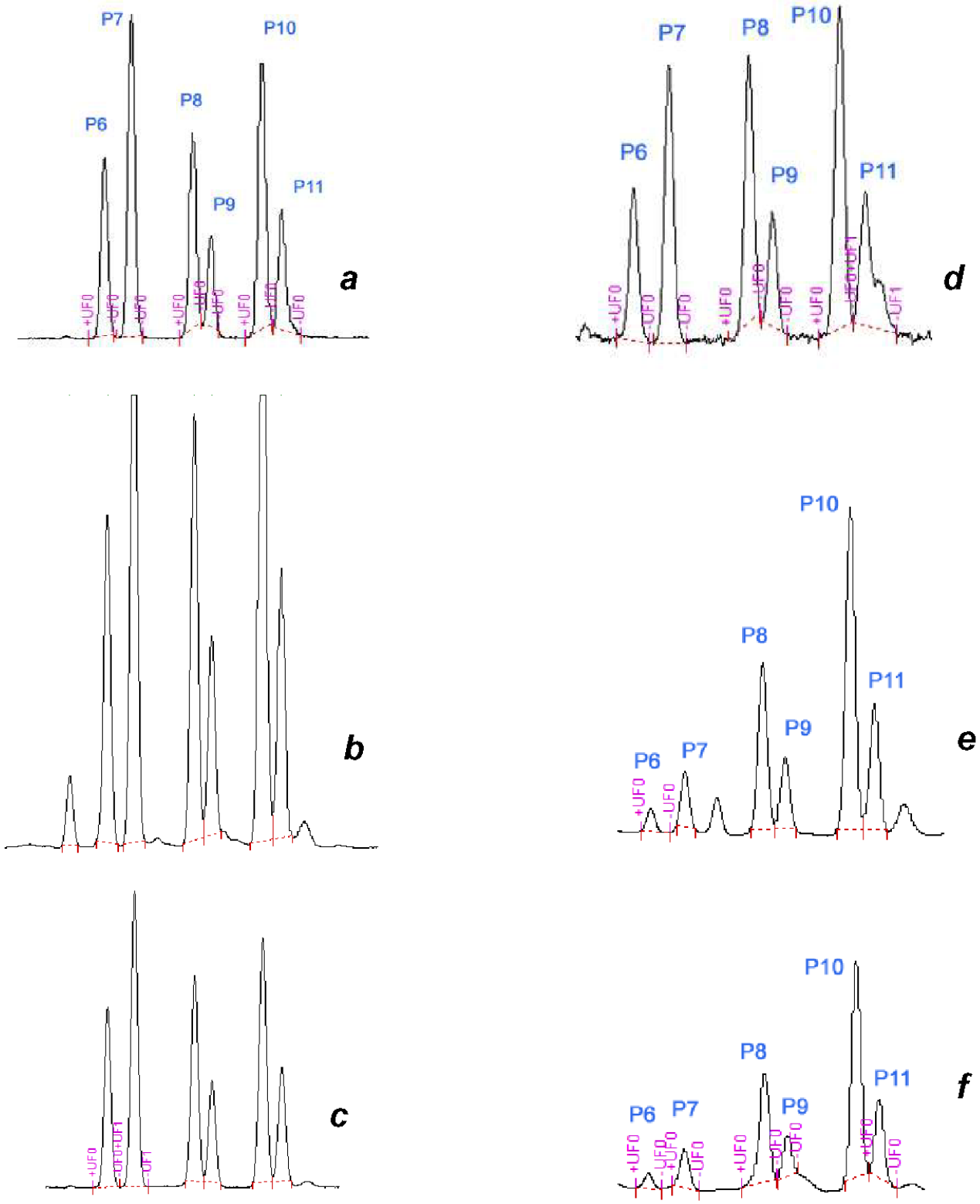

Figure S12. Chromatograms of products **P6**–**P11** (see Fig. S11) of the reaction mixtures obtained in the reactions of methycyclohexane with H_2O_2 (*a*, *b*, *c*) and TBHP (*d*, *e*, *f*) catalyzed by the $Os_3(CO)_{12}$/py system (*a*) and complexes **1a** (*b*, *e*) and **2** (*c*, *f*). The chromatogram for the oxidation with TBHP in the absence of any catalyst is also shown (*d*).

Product **I**

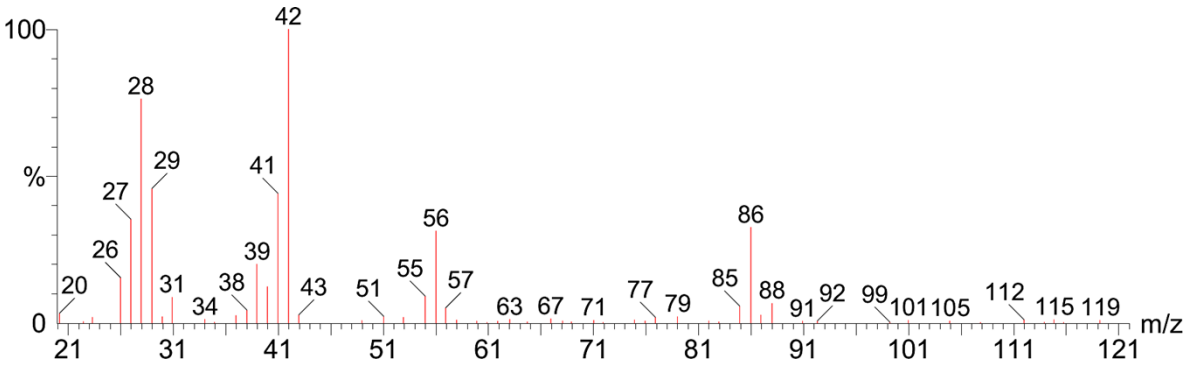

Product **II**

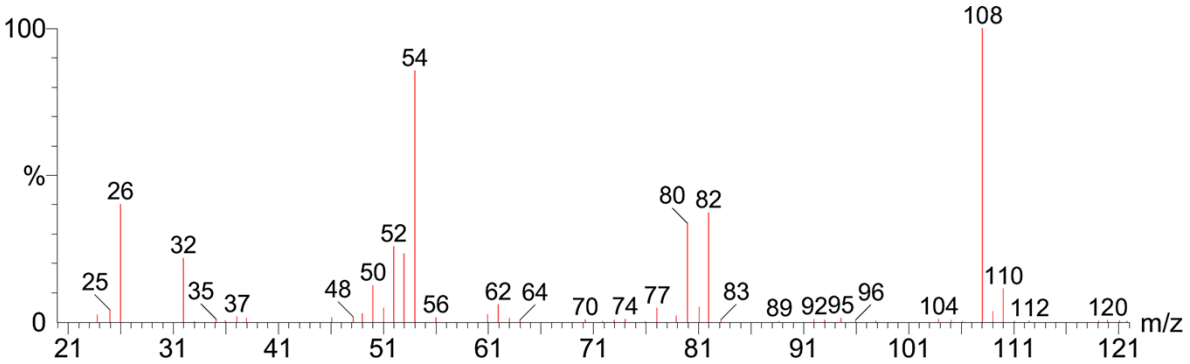

Product **III**

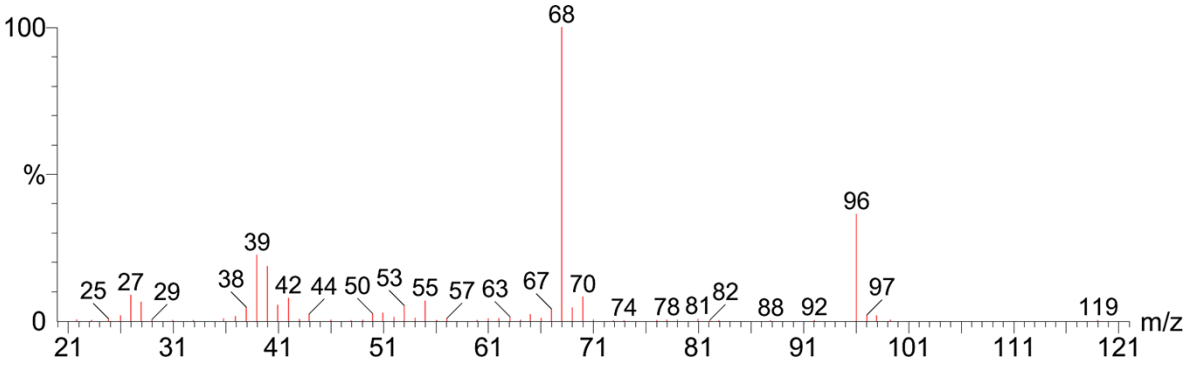

Product **IV**

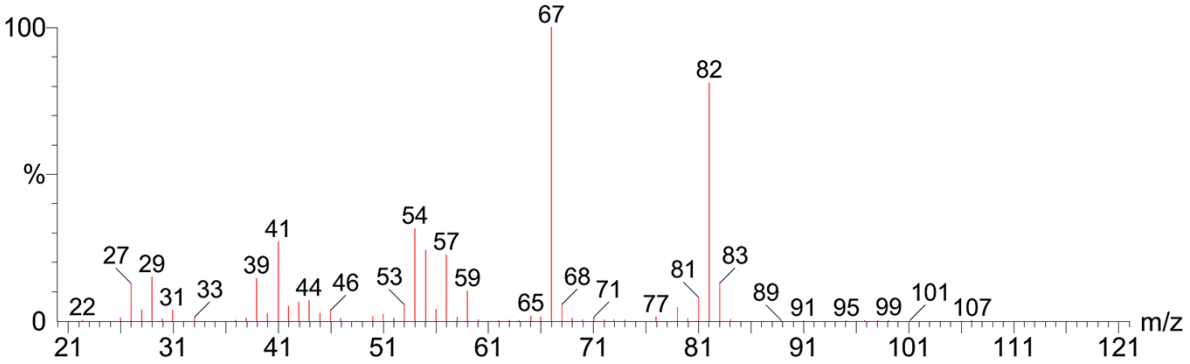

Product **V**

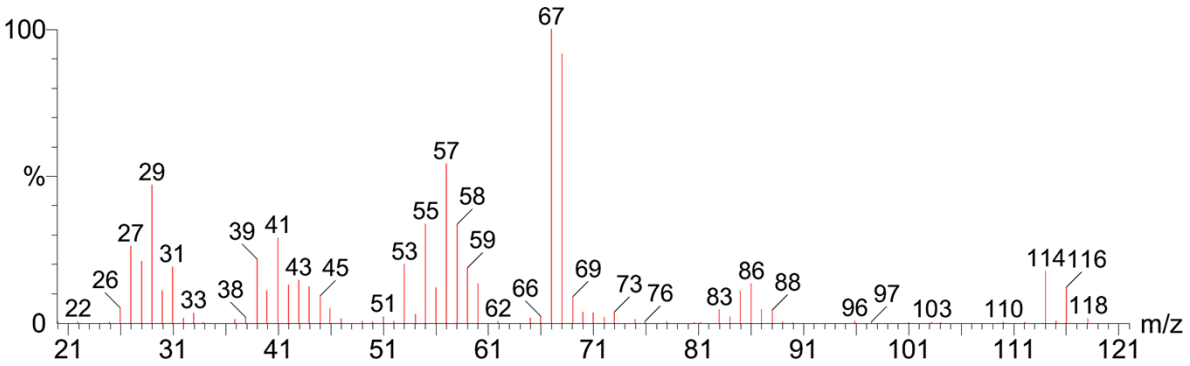

Product **VI**

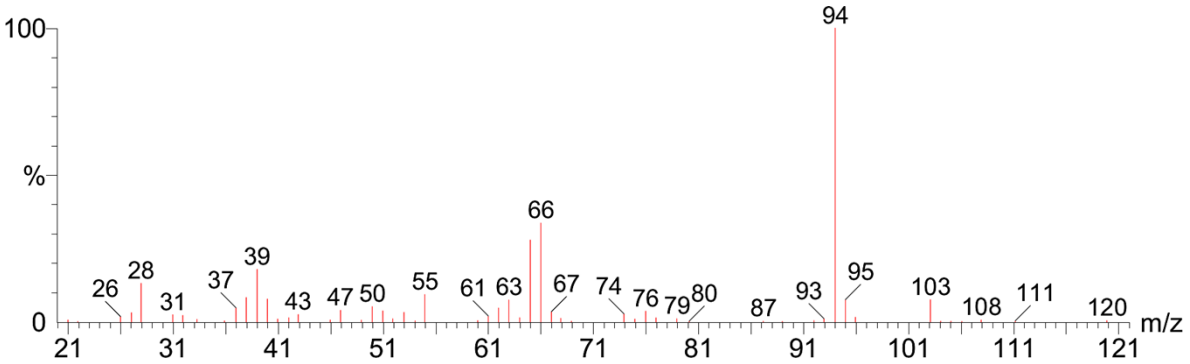

Product **VII**

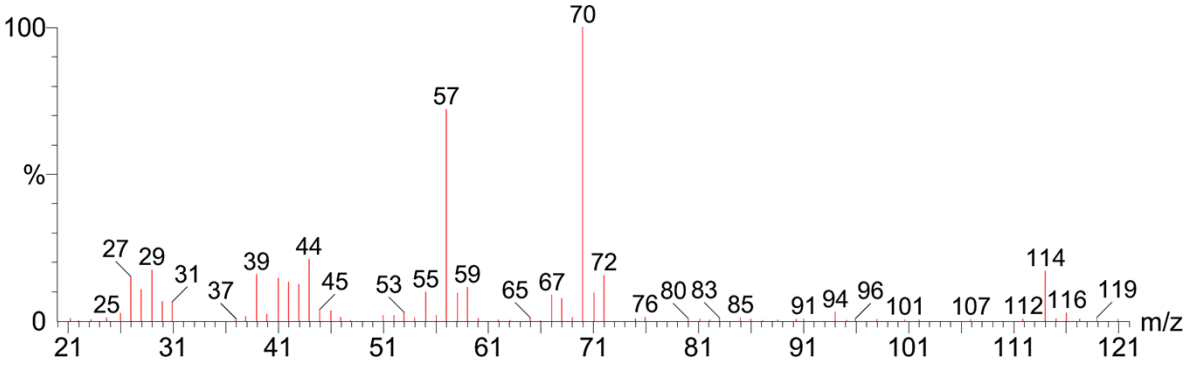

Product **VIII**

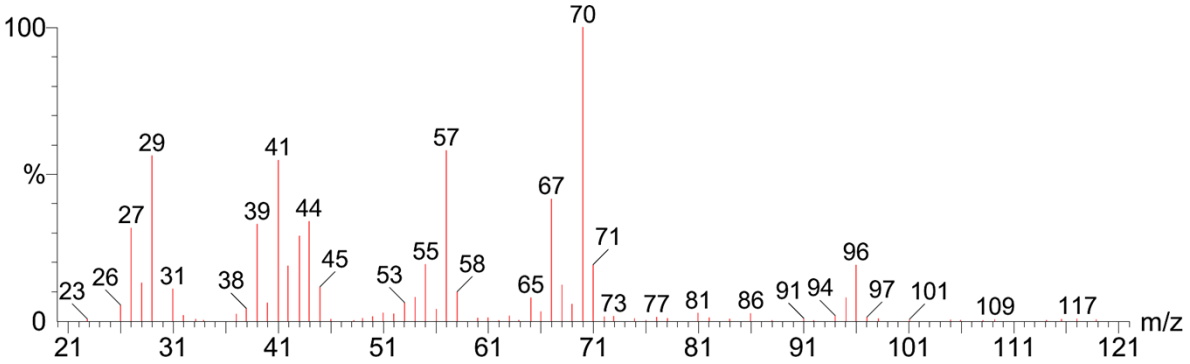

Product **IX**

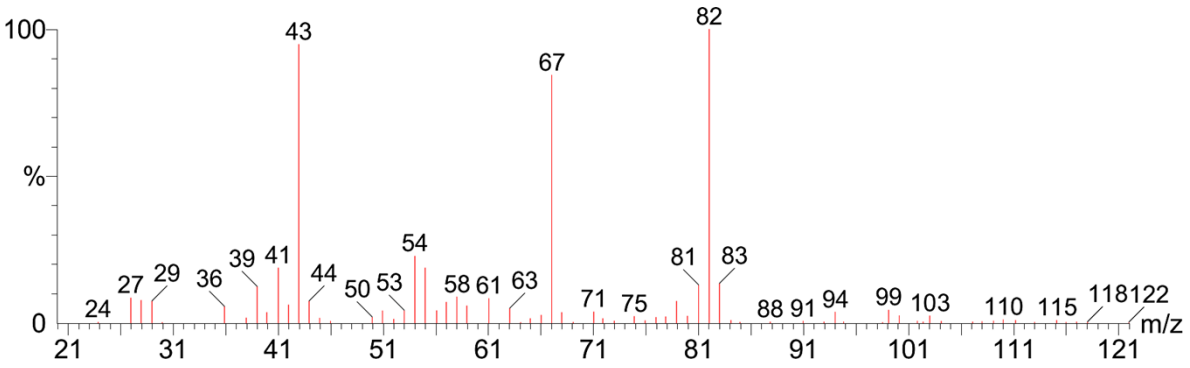

Product **X**

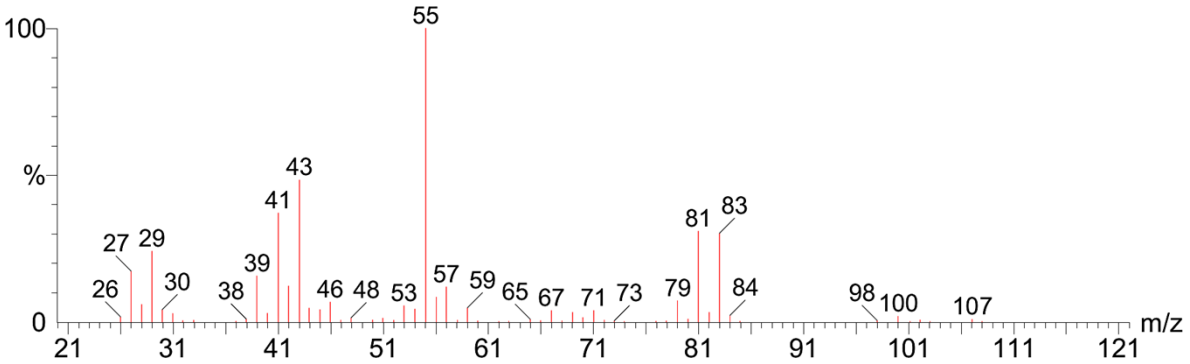

Product **XI**

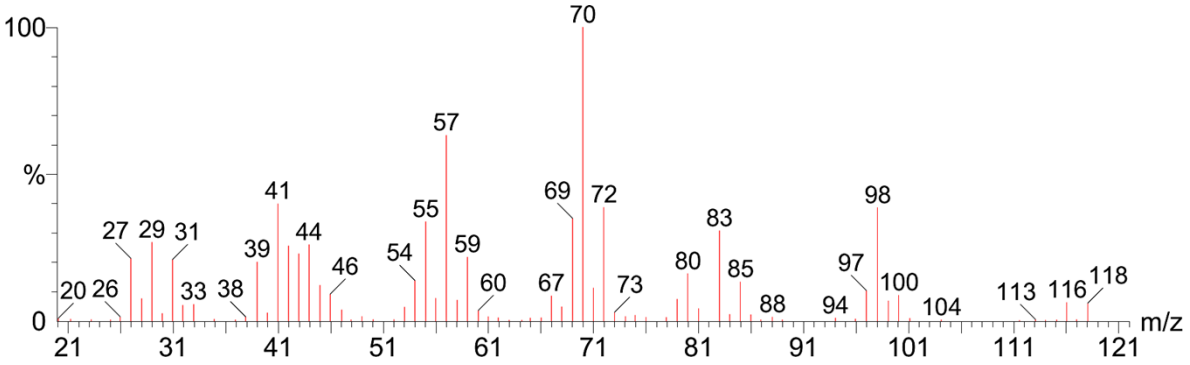

Product **XII**

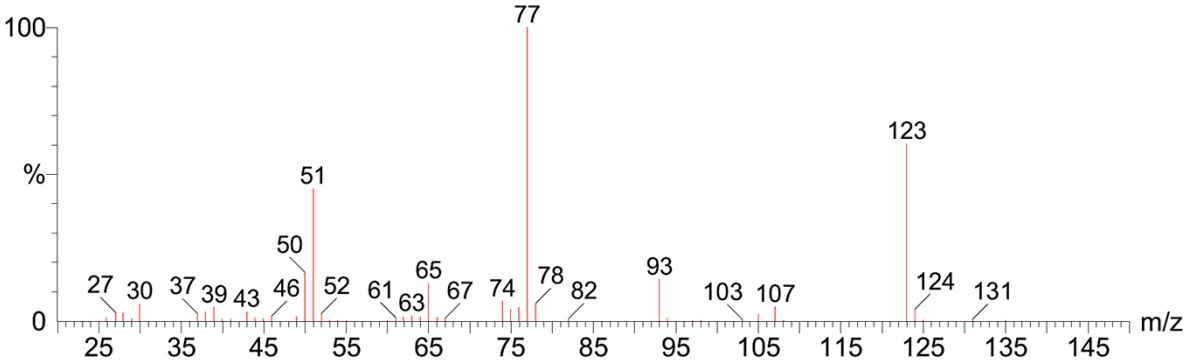

Product **XIII**

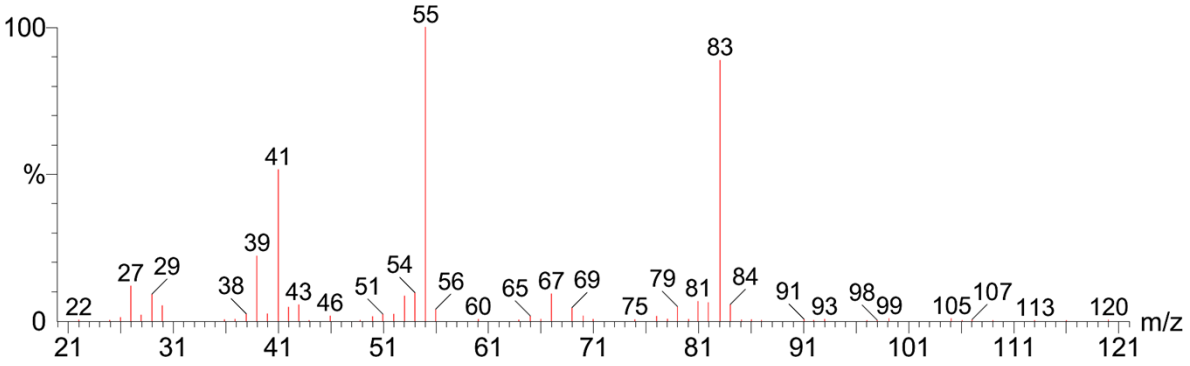

Product **XIV**

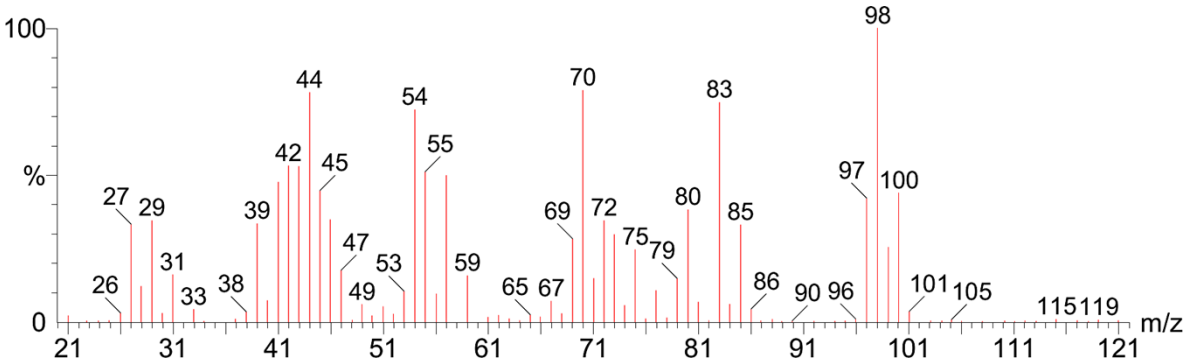

Product **XV**

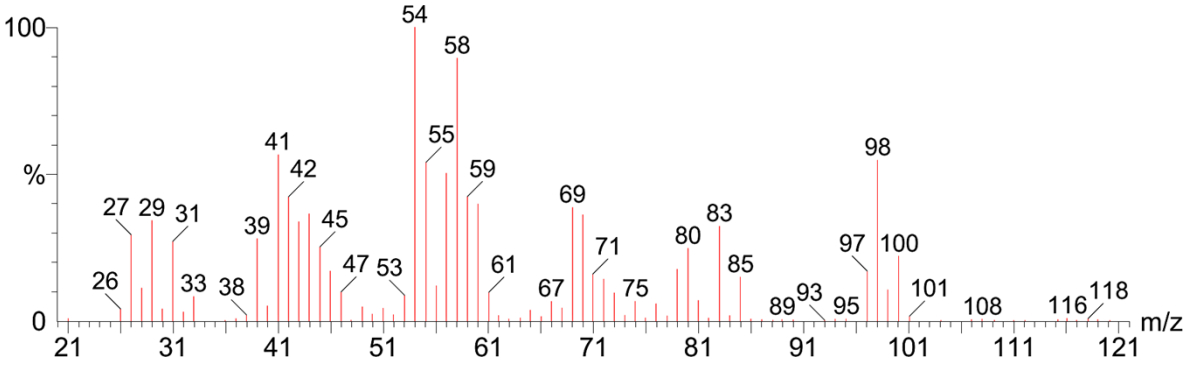

Product **XVI**

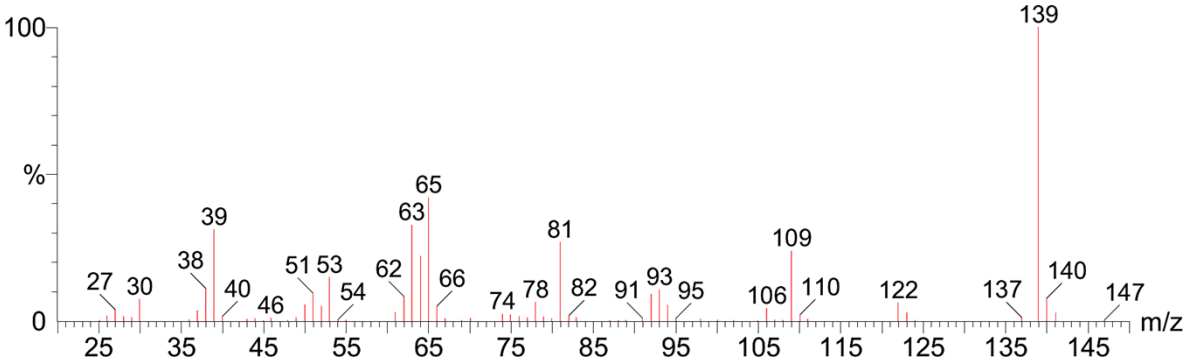

Product **XVII**

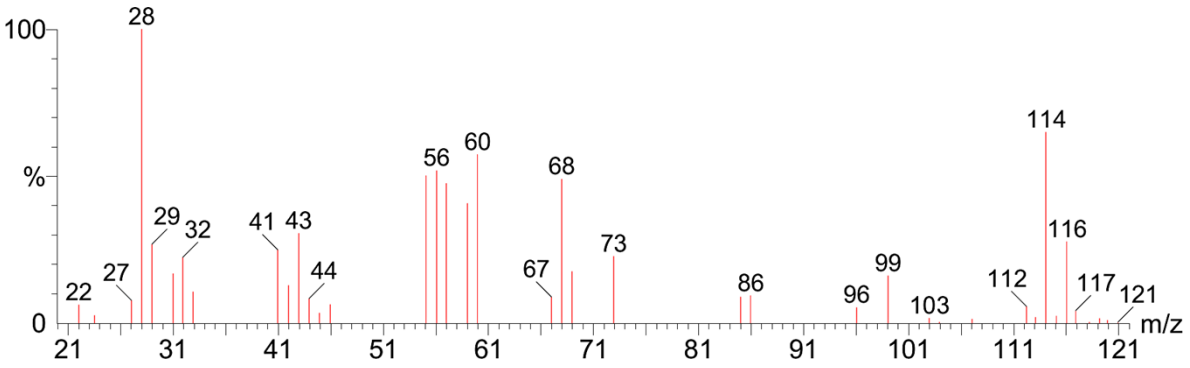

Product **XVIII**

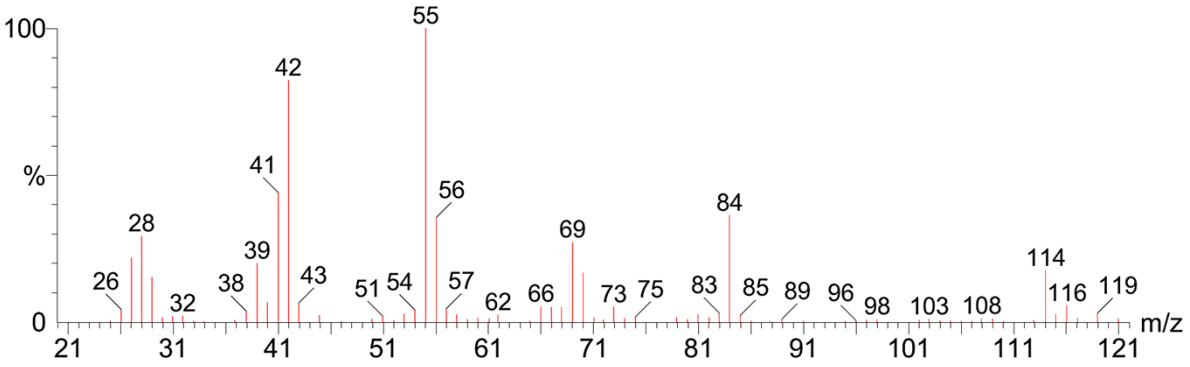

Figure S13. Electron ionization mass spectra of the products **I**–**XVIII** (see Fig. 12 in the main text).

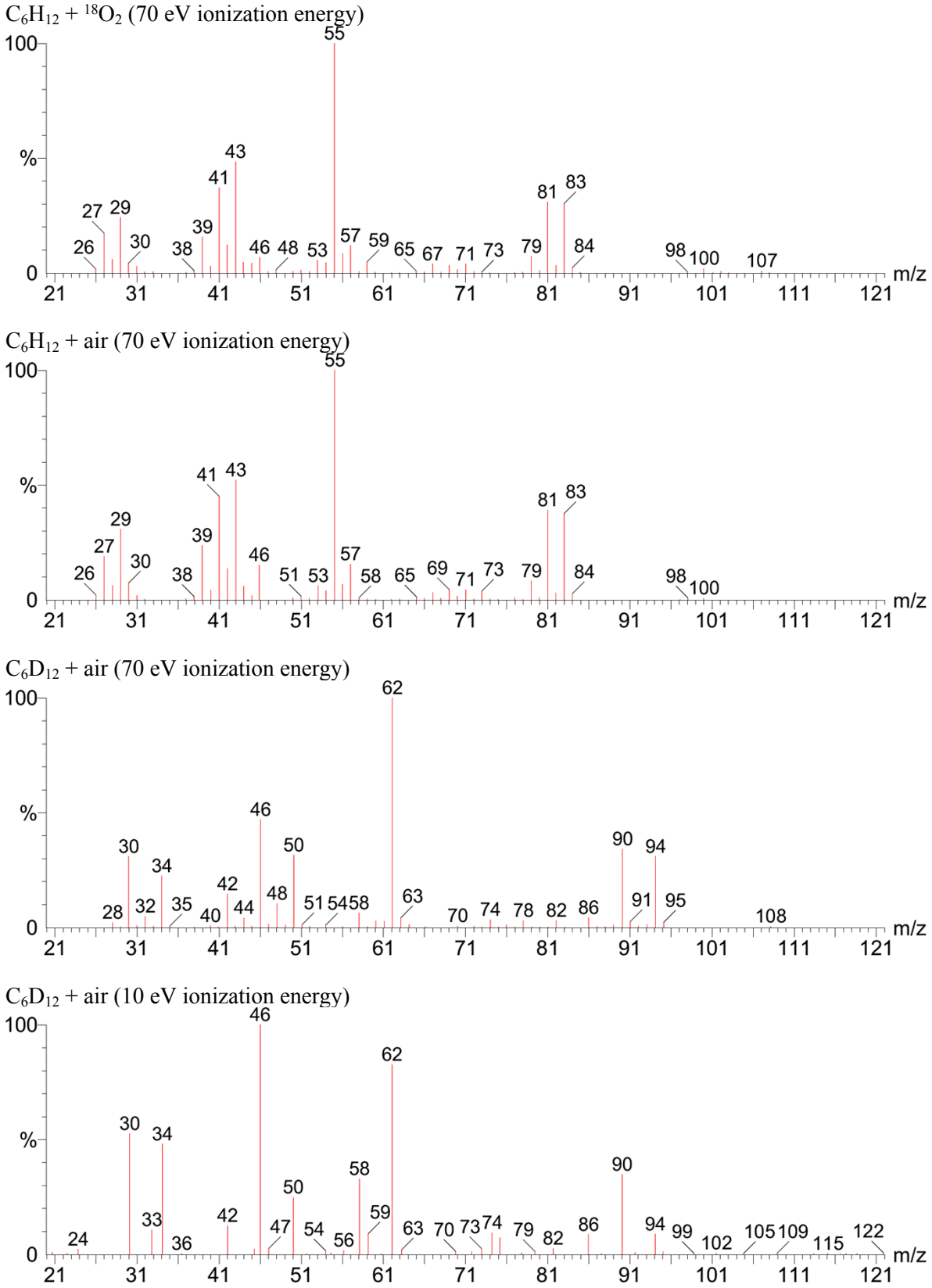

Figure S14. Electron ionization mass spectra of the product **X** (see Fig. 12 in the main text) under specified conditions (substrate, atmosphere and ionization energy).